Available online at www.sciencedirect.com
ScienceDirect
Ceramics International 36 (2010) 1297–1302
CERAMICS INTERNATIONAL
www.elsevier.com/locate/ceramint

Erosion behaviour of B_4C-based ceramic composites

Changxia Liu *, Junlong Sun

Key Laboratory of Advanced Manufacturing and Automation Technology, Ludong University, Yantai 264025, Shandong Province, PR China

Received 9 February 2009; received in revised form 16 October 2009; accepted 29 December 2009
Available online 29 January 2010

Abstract

In this paper, TiO_2 was introduced into boron carbide and B_4C-based ceramic composites were obtained by uniaxial hot pressing. The mechanical properties, relative density and erosion behaviour of B_4C-based ceramic composites were investigated. X-ray analysis showed that the fabricated composites were composed of B_4C, TiB_2 and C phases. SEM technique was employed to observe the original polished surfaces and the eroded surfaces of B_4C-based ceramic composites. The effect of impingement angle, impact velocity of SiC erodent particle, relative density and phase ratio on the erosion rate of B_4C-based ceramic composites was determined. It was found that the erosion rate of B_4C-based ceramic composites increased with increasing of impingement angle and erodent particle velocity. The relative density and phase ratio influenced the erosion rate of B_4C-based ceramic composites significantly by influencing their mechanical properties.

Keywords: A. Hot pressing; B_4C; TiB_2; Erosion behaviour; Microstructures

1. Introduction

Erosion is a serious problem in many engineering systems, such as jet turbines, pipelines and valves used in slurry transportation, cyclone generators and fluidized bed sand boilers [1–3]. Ceramic matrix composites possess attractive properties, these include high hardness, low density, good chemical stability, high corrosion resistance and temperature tolerance, making them useful for advanced structural and tribological applications [4–6]. Boron carbide (B_4C) has excellent hardness, a high melting point, low specific weight and great resistance to chemical agents at room temperature, so it is currently used in high technology industries for such applications as blasting nozzles, light weight armors and high temperature thermoelectric conversion. Abrasive air-jet nozzles made of boron carbide of high relative density provides a long life owing to excellent wear resistance compared with other nozzle materials [7–8].

Although there is considerable interesting on the erosion wear of ceramic materials, little work has been reported on the erosion behaviour of $B_4C/TiB_2/C$ ceramic composites. In this study, the erosion wear of $B_4C/TiB_2/C$ ceramic composites with different mechanical properties and microstructures were investigated using abrasive air-jets. The factors that influence the erosion wear behaviour of $B_4C/TiB_2/C$ ceramic composites were analyzed and the erosion wear mechanisms were determined by microstructural analysis by comparison of eroded and polished surfaces.

2. Experimental procedure

Commercial B_4C powder with a particle size of 3–5 μm was used as the starting materials (produced by the second erodent material factory of Peony River, Heilongjiang province, China). TiO_2 with 1–2 μm particle size (produced by Shanghai Taibai Product of Chemistry and Industry Co., Ltd.) were used as additives. B_4C and TiO_2 were milled at certain proportions as indicated in Table 1. Milling was carried out for 100 h in alcohol using a vibratory ball mill with cemented carbide (WC) balls. The milled powders were then washed in 10 mol.% hydrochloric acid to remove metal-mill media impurities. The average particle size of the final milled powders was less than 1.5 μm. After drying the powder, densification of the compacted powder was achieved in a graphite die by uniaxial hot-press sintering at 1900 °C, at a pressure of 35 MPa in a N_2 atmosphere for 50 min. The diameter and thickness of the hot-press sintered green compacts were 50 mm and 6 mm,

* Corresponding author. Tel.: +86 15866472136.
E-mail address: hester5371@yahoo.com.cn (C. Liu).

0272-8842/$36.00
doi:10.1016/j.ceramint.2009.12.024

Table 1
Starting compositions of the samples.

Samples	Starting compositions (wt.%)	
	B_4C	TiO_2
NT1	96	4
NT2	92	8
NT3	88	12

respectively. The final relative densities were determined using the Archimedes method and are shown in Table 2.

Some of the sintered compacts were cut into bars for measuring the mechanical properties while the remainder was used for erosion tests. Standard test bars (3 mm × 4 mm × 36 mm) were obtained through rough grinding, finish diamond grinding, and finally polished to a 0.1 μm finish. Three-point-bending mode was used to measure the bending strength using an electronic universal experimental instrument (produced by Jinan TEST Co., Ltd.) with a span of 20 mm at a crosshead speed of 0.5 mm/min. At least twelve specimens were tested for each series of composition in air at room temperature.

Vickers hardness was measured on the polished surfaces with a load of 9.8 N for 5 s using a micro-hardness tester (produced by Shanghai Hengyi electronic testing instrument corporation). Fracture toughness measurements were performed using indentation method. For the fracture toughness determinations the indentations on polished surfaces were generated by the Vickers micro-hardness tester with a diamond pyramid indenter, at a load of 196 N and a loading time of 30 s. The formula proposed by Cook and Lawn [9] was used to calculate the final fracture toughness. Hardness and fracture toughness data were determined using at least 10 indentations on polished surfaces with an Ra of 0.1 μm for each specimen.

Erosion tests were performed under ambient conditions of temperature and humidity over a period of 30 min with an abrasive air-jet machine tool (produced by Qingdao SHIYONG hardware machinery Co., Ltd.). The erodent material used in this study was 150–180 μm SiC powder, of 3.15 g/cm^3 density, 32.8–34.0 GPa hardness and ≥99% purity. NT1, NT2 and NT3 disc specimens with a diameter of 50 mm and thickness of 6 mm were carried out for erosion tests, and the test specimens were located 10 mm from nozzle orifice for all impingement angles. Impingement angles of 15°, 30°, 45°, 60°, 75°and 90° were adopted and the particle velocities of 30 m/s, 45 m/s, 60 m/s and 75 m/s were used. The particle velocity was controlled by means of the compressed air pressure and measured using the rotating double disk technique [10]. Three specimens at each test condition were adopted in order to minimize data scattering and decrease the relative error.

Volume erosion rate was used to rank the erosion behaviour of the B_4C-based ceramic composites, and was calculated using the following equation

$$V = \frac{M}{\rho \times M_p} \quad (1)$$

where V was the volume erosion rate (mm^3/g) of the tested disc specimen, M and ρ were the mass loss (g) and real density (g/mm^3) of the tested disc specimen, respectively, and M_p was the mass (g) of erodent particles used during the test. Mass loss of the tested disc specimen was measured using an analytical balance with an accuracy of 0.1 mg. Prior to weighting the specimens were cleaned using an ultrasonic bath with distilled water for about 10 min. The mass of erodent used in each test is 30 kg. The erodent can be used circularly in each test and the used erodent in previous test will be replaced by new erodent when new test is carried on.

The original polished surfaces and the eroded surfaces of NT2 and NT3 disc specimens were examined in a scanning electron microscope (HITACHI S-570). The phases and phase content for the fabricated B_4C-based ceramic composites were determined using an XRD (D/max-2400).

3. Result and discussion

3.1. X-ray diffraction phase analysis

The X-ray diffraction analysis data of the NT2 specimen hot-pressed at 1900 °C for 50 min is shown in Fig. 1. It was observed that B_4C, TiB_2 and C phases were present, and no trace of TiO_2 phases was detected. The final relative wt.% phase compositions of the three hot-press sintered samples are shown in Table 2.

TiO_2 reacted with B_4C by the following equations [11]

$$B_4C + 2TiO_2 \rightarrow 2TiB_2 + CO_2\uparrow + O_2\uparrow \quad (2)$$

$$B_4C + 2TiO_2 \rightarrow 2TiB_2 + C + 2O_2\uparrow \quad (3)$$

Based on thermodynamic analysis of chemical reactions, the values of ΔG^θ, the Gibbs free energy for Eqs. (2) and (3), were less than zero, which indicated that Eqs. (2) and (3) could occur under these experimental conditions. It is generally agreed that

Table 2
The final compositions, grain size, relative density and mechanical properties of B_4C-based ceramic composites.

Specimens	Relative compositions (wt.%)			Mechanical properties			Grain size (μm)	Relative density (%)
	B_4C	TiB_2	C	Vickers hardness (GPa)	Flexural strength (MPa)	Fracture toughness (MPa m$^{1/2}$)		
NT1	95.7	3.5	0.8	26.3 ± 1.6	435 ± 21	4.1 ± 0.4	5.0	93.6 ± 0.8
NT2	91.8	5.2	3.0	27.6 ± 1.0	551 ± 14	5.2 ± 0.2	3.0	96.2 ± 0.6
NT3	87.4	7.0	5.6	25.4 ± 1.8	553 ± 20	3.9 ± 0.5	2.5	95.5 ± 0.5
Pure B_4C [15]	100	0	0	18.1 ± 2.0	240 ± 25	2.5 ± 0.7	–	86.4 ± 0.5

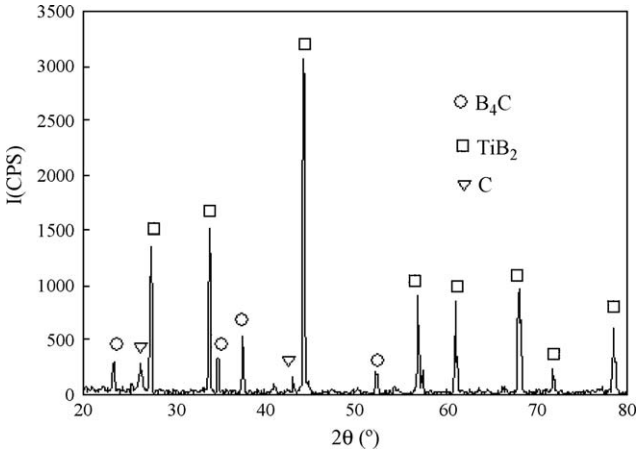

Fig. 1. X-ray diffraction analysis of the NT2 specimen (1900 °C, 50 min).

the boron oxide (B_2O_3) impurity in B_4C raw material exists as a compact layer that retards the sintering of B_4C-based ceramic composites, for boron oxide impurity can generate boron suboxides by in combination with boron carbide [12]

$$B_4C + 5B_2O_3 \rightarrow 7B_2O_2 + CO \quad (4)$$

Vapor phase, formed by the volatile boron suboxides, are effective in transportation of the matrix and the additives. Vapor phase transport, however, can reduce the driving force for sintering and increase the average diffusion distance, and merely redistributes matter to the necks between sintering powders rather than promoting a grain center approach which is mandatory for shrinkage [12]. Carbon is considered as a sintering additive [13,14], and the addition of carbon is an effective method to enhance the sinterability of B_4C-based ceramic composites, as carbon can react to eliminate boron oxide impurity. So the following reaction takes place during the hot-press sintering process [12]

$$2B_2O_3 + 7C \rightarrow B_4C + 6CO \quad (5)$$

The elimination of this boron oxide impurity will accelerate the densification of hot-press sintered B_4C-based ceramic composite.

3.2. Mechanical properties

The mechanical properties of the hot-press sintered B_4C-based ceramic composites are shown in Table 2. All the specimens in the present tests had relative densities greater than 93.6%, while that of monolithic boron carbide, fabricated using the same sintering parameters in our previous study, was 86.4% [15]. The improved relative density of B_4C-based ceramic composites may be due to the elimination of the boron oxide impurity and the reaction between boron carbide and TiO_2.

Kim et al. [16] have observed that the mechanical properties, such as bend strength, fracture toughness, hardness and elastic modulus, of sintered B_4C-based ceramic composites with Al_2O_3 improved with the increased relative density. Compared with monolithic boron carbide, fabricated under the same conditions in our previous study, with hardness of 18.1 GPa, strength of 240 MPa and toughness of 2.5 MPa $m^{1/2}$ [15], the hot-press sintered B4C-based ceramic composites of the present study exhibited better mechanical properties, which may be mainly due to their increased relative density, see Table 2. The mechanical properties of hot-press sintered B_4C-based ceramic composites in our present study, however, were not only affected by their relative density, but also by their phase ratio and grain size. As can be seen in Table 2, the relative density of the NT2 specimen reached the highest value of 96.2%, which also had the highest Vickers hardness. The grain size of the fabricated composites, measured by the linear intercept technique, decreased with the increasing TiB_2 and C content, which contributed to the improved flexural strength of the NT2 and NT3 specimen. The fracture toughness of the fabricated composites increased with the increase of TiB_2 and C content up to the NT2 concentration and then decreased with further addition of TiB_2 and C. Comparing NT2 with NT3 specimen, one could assume that the performance of the NT3 specimen was reduced maybe due to the high remnant C. Therefore, an optimal phase ratio may contribute to the improved mechanical properties of the fabricated B_4C-based ceramic composites.

It was concluded that the NT2 specimen showed better overall performance, which may be mainly due to the highest relative density, the refining of the grain size and the appropriate phase ratio of the composite. The hardness, flexural strength and fracture toughness of the NT2 specimen reached 27.6 GPa, 551 MPa and 5.2 MPa $m^{1/2}$, respectively, which was an improvement of 52.5%, 129.5% and 108%, respectively, with respect to monolithic boron carbide hot-press sintering using the same conditions [15].

3.3. Effect of impact angle and velocity

Fig. 2 illustrates the dependence of the erosion rate on the impact angle for the hot-press sintered B_4C-based ceramic composites eroded by SiC particles at velocity of 60 m/s. As can be seen from Fig. 2, the erosion rate of B_4C-based ceramic composites increased with increasing impact angle and the

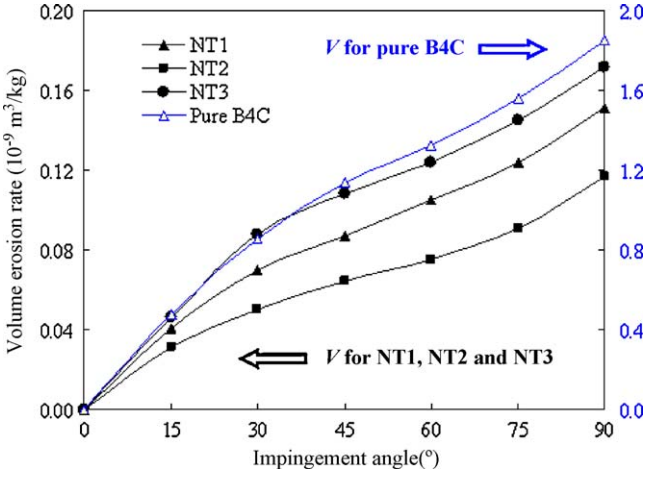

Fig. 2. Dependence of the erosion rate on the impact angle for B_4C-based ceramic composites.

maximum erosion rate occurred at 90°. The erosion rate for all specimens was approximately four times greater at an impact angle of 90° than at 15°. Wear resistant engineering materials according to their response to erosion can be grouped traditionally into brittle and ductile materials [1–2]. The group in which plastic deformation predominates and which displays maximum erosion rate at low-impact angles is usually known as ductile material (e.g. metals), while the group in which fracture dominates and which displays maximum erosion rate at normal impact angle is usually known as brittle material (e.g. ceramics) [1]. Erosion tests as a function of impact angle showed that the fabricated B_4C-based ceramic composites displayed a typical brittle character.

The effect of erodent particle velocity on the erosion rate of B_4C-based ceramic composites at 90° is shown in Fig. 3. For all the specimens, the erosion rate increased with the increase in particle impact velocity. Regression analysis shows that a power law provides the best empirical fit to the experimental data. A power law exponent for particle velocity which varied from 2.4 to 2.6 was determined for the B_4C-based ceramic composites eroded here. The range observed is similar to that most-cited in the literature [2,17,18].

It can be seen from Figs. 2 and 3 that NT1, NT2 and NT3 specimens showed low erosion rate of magnitude 10^{-10} m^3/kg, smaller than that of pure B_4C (10^{-9} m^3/kg). The erosion rate of pure B_4C was about 9 times larger than that of NT1, NT2 and NT3 specimens. This is mainly due to the improved mechanical properties and increased relative density of NT1, NT2 and NT3 specimens (Table 2). For NT1, NT2 and NT3 specimens, a similar trend was found from Figs. 2 and 3 that the erosion rate for NT3 specimen showed the highest value while that of NT2 specimens was the lowest. The hardness and toughness of NT2 specimen were 27.6 GPa and 5.2 MPa $m^{1/2}$, which were the highest values within the set of the specimens, and that of NT3 were 25.4 GPa and 3.9 MPa $m^{1/2}$, which were the lowest. Therefore, the erosion rate of NT2 specimen was the lowest, and that of NT3 specimen was the highest. As previously stated, the existence of an appropriate amount of free C and TiB_2 in B_4C-based ceramic composites can contribute to the increased relative densities and mechanical properties, which may result in the improved erosion properties of the NT2 specimen. However, the excess of free C in B_4C-based ceramic composites can lead to the weak grain boundaries, and result in the diminished erosion properties as seen in the NT3 specimen. In other words, another factor that lead to the improved erosion properties of the NT2 specimen may be the optimal phase ratio in the composite. The relative density of the NT3 specimen was 95.5%, which was higher than that of the NT1 specimen (93.6%), so there should be a trend that the NT3 specimen showed a lower value of erosion rate than the NT1 specimen when comparing relative density of the two specimens. However an inverse trend became and the erosion rate of NT3 specimen was higher than that of the NT1 specimen. The content of in situ formed TiB_2 and C in NT3 specimen was higher than that in NT1 specimen, higher content of TiB_2 and C, with lower hardness than the B_4C matrix, may lead to the lower hardness of the NT3 specimen, although with higher relative density than the NT1 specimen (Table 2). Therefore, the content of TiB_2 and C may influence the erosion rate of the hot-press sintered B_4C-based ceramic composites by influencing their hardness. As a result, it can be concluded that phase ratio has more significant influence on the overall erosion performance of B_4C-based ceramic composites than density.

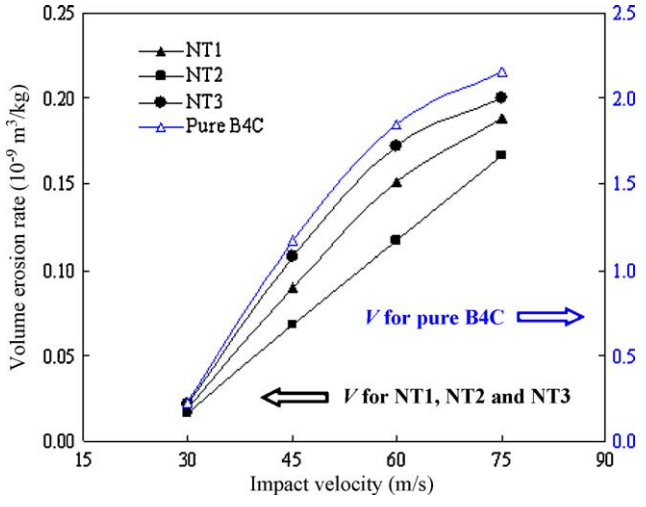

Fig. 3. Effect of erodent particle velocity on the erosion rate of B_4C-based ceramic composites at 90°.

3.4. Microstructural examination of the original polished and eroded surfaces

SEM photomicrographs of original polished surface of the NT2 and NT3 specimens are shown in Figs. 4 and 5. The dark area was identified by EDX analysis to be B_4C and the light area was TiB_2 and free C. It was noted that TiB_2 and free C were uniformly distributed throughout NT2 and NT3 specimens and

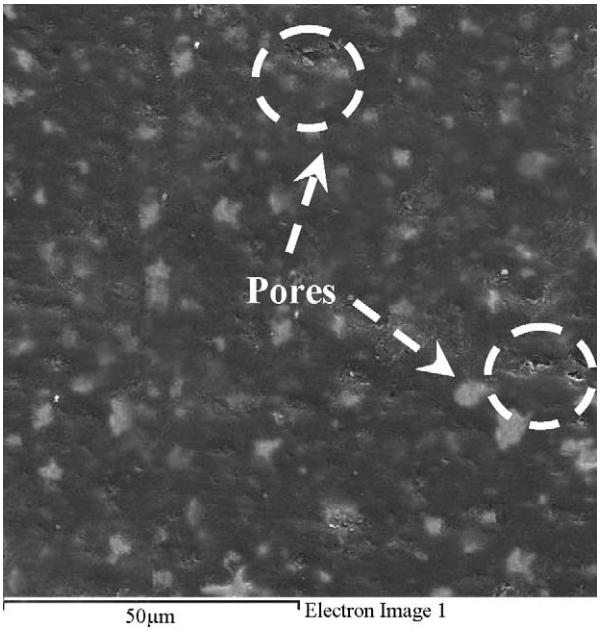

Fig. 4. SEM photomicrographs of polished surface of NT2 specimen.

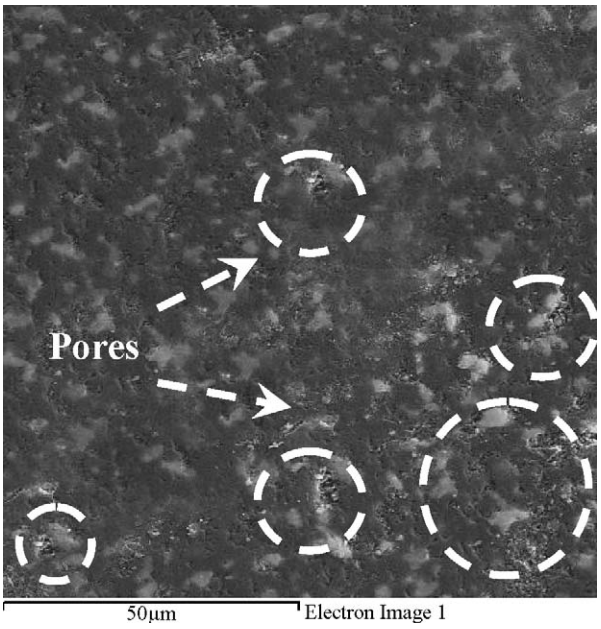

Fig. 5. SEM photomicrographs of polished surface of NT3 specimen.

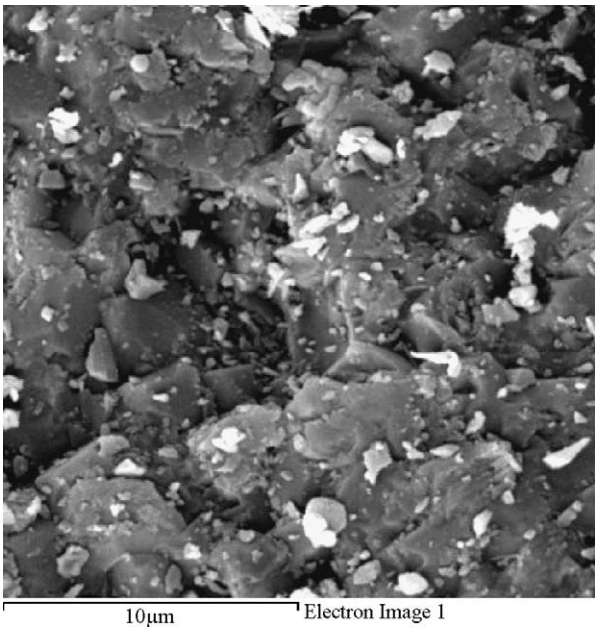

Fig. 7. An eroded area of NT2 specimen at an impingement angle of 90°.

a few pores (marked with circle in Figs. 4 and 5) were also observed. The mean pore size of the NT2 and NT3 specimens was about 1 μm. There appeared more light areas and more porosity in NT3 specimen than that in NT2 specimen, which could explain the higher relative densities and mechanical properties of NT2 specimen.

Previous researchers have pointed out that the ceramic materials exhibited both the brittle mode of fracture as well as the semibrittle mode of plastic deformation [1–3,5,19]. Figs. 6 and 7 show the final eroded surfaces of the NT2 specimen, eroded at impingement angles of 30° and 90°. At 30° impact it was evident that erosion damage was dominated by plastic deformation for the NT2 specimen (Fig. 6), while at 90° impact, grain ejection by fracture was the main material removal mechanism and there were fewer and smaller plastically deformed regions present (Fig. 7).

Figs. 8 and 9 show the final eroded surface of the NT3 specimen eroded at impingement angles of 30° and 90°. For the NT3 specimen it was found that at 30°, erosion damage was dominated by both grain ejection and plastic deformation (Fig. 8), while at 90° grain ejection was the main material removal mechanism and there were fewer deformed regions (Fig. 9). The difference in erosion rate between NT2 and NT3 specimen may be accounted for by the different material removal mechanism, which may be mainly due to the different phase ratio in the composites.

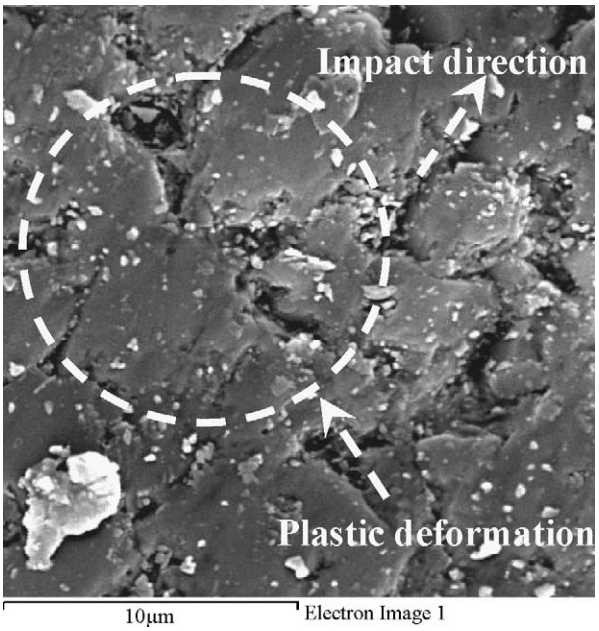

Fig. 6. An eroded area of NT2 specimen at an impingement angle of 30°.

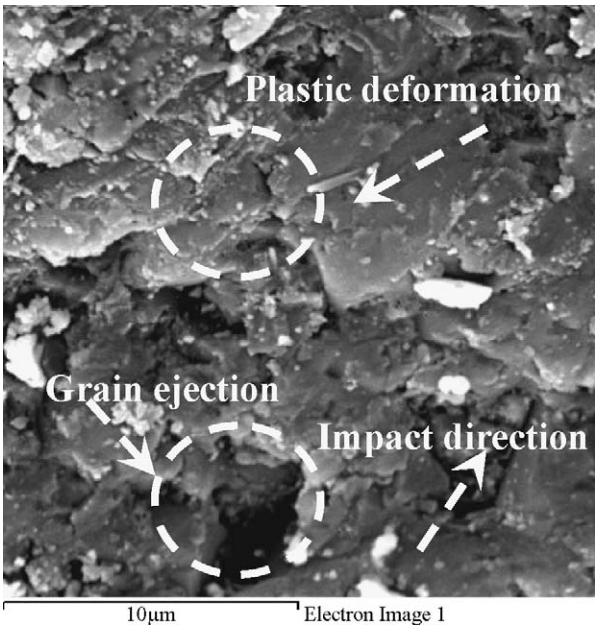

Fig. 8. An eroded area of NT3 specimen at an impingement angle of 30°.

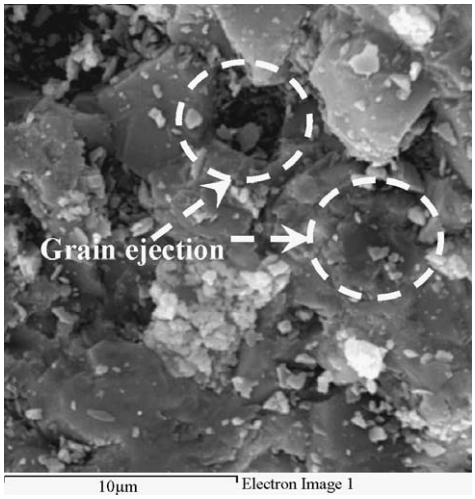

Fig. 9. An eroded area of NT3 specimen at an impingement angle of 90°.

4. Conclusions

B_4C-based ceramic composites were fabricated by hot-press sintering and then subjected to an air-jet impact erosion test using SiC media. Post-erosion analysis has been carried out. The following conclusions were made:

1. The fabricated B_4C-based ceramic composites consisted of TiB_2, B_4C and C phases after hot-press sintering, which indicated that all the initially introduced TiO_2 reacted with B_4C during the hot-press sintering process.
2. Results of the erosion tests indicated the NT2 specimen was the most erosion resistant, while the NT3 specimen was the least resistant. For NT1, NT2 and NT3 specimens, the erosion rate at 90° impact angle was approximately four times greater than that at 30° impact angle. A power law exponent which varied from 2.4 to 2.6 was achieved for SiC particle velocity B_4C-based ceramic composite erodes.
3. In all samples, erosion damage was dominated by plastic deformation at 30° impingement angles, while at 90° impact, a brittle fracture mechanism resulting in which grain ejection was the main material removal mechanism.
4. The erosion rate at all angles correlated directly with the relative density of the composite and less so with the other physical properties, although sample NT2 also had the highest mean physical properties of all compositions and densities.

Acknowledgement

The work described in this paper is supported by the Specialized Personnel Invitation Rewards of Ludong University (No. LY20074303 and No. LY20074302).

References

[1] Q. Fang, H. Xu, P.S. Sidky, M.G. Hocking, Erosion of ceramic materials by a sand/water slurry jet, Wear 224 (1999) 183–190.
[2] Y. Zhang, Y.-B. Cheng, S. Lathabai, Erosion of alumina ceramics by air- and water-suspended garnet particles, Wear 240 (2000) 40–51.
[3] G.E. D'Errico, S. Bugliosi, D. Cuppini, Erosion of ceramic and cermets, J. Mater. Process. Technol. 118 (2001) 448–453.
[4] L. Changxia, Z. Jianhua, Z. Xihua, S. Junlong, H. Yujing, Addition of Al-Ti-C master alloys and ZrO_2 to improve the performance of alumina matrix ceramic materials, Mater. Sci. Eng. A 426 (2006) 31–35.
[5] J.G. Chacon-Nava, S.D. delaTorre, A. Martinez-Villafane, Erosion of alumina and silicon carbide at low-impact velocities, Mater. Lett. 55 (2002) 269–270.
[6] L. Changxia, Z. Jianhua, S. Junlong, Z. Xihua, Pressureless sintering of large-scale fine structural alumina matrix ceramic guideway materials, Mater. Sci. Eng. A 444 (2007) 58–63.
[7] D. Jianxin, S. Junlong, Sand erosion performance of B4C based ceramic nozzles, Int. J. Refract. Met. Hard Mater. 26 (2008) 128–130.
[8] D. Jianxin, L. Lili, Z. Jinliong, S. Junlong, Erosion wear of laminated ceramic nozzles, Int. J. Refract. Met. Hard Mater. 25 (2007) 263–270.
[9] R.F. Cook, B.R. Lawn, A modified indentation toughness technique, J. Am. Ceram. Soc. 66 (11) (1983) 200–201.
[10] I.M. Hutchings, Solid particle wear testing, ASM Int. 8 (2000) 343–344.
[11] S. Junlong, Development of new B_4C composite ceramic nozzle and study on its erosion mechanisms, Ph.D. Dissertation, Shandong University, 2007.
[12] L.S. Sigl, Processing and mechanical properties of boron carbide sintered with TiC, J. Eur. Ceram. Soc. 18 (11) (1998) 1521–1529.
[13] K.A. Schwetz, L.S. Sigl, L. Pfau, Mechanical properties of injection molded B_4C-C ceramics, J. Solid State Chem. 133 (1997) 68–76.
[14] F. Thevenot, Boron carbide-a comprehensive review, J. Eur. Ceram. Soc. 6 (4) (1990) 205–225.
[15] S. Junlong, L. Changxia, D. Caiyun, Effect of Al and TiO_2 on sinterability and mechanical properties of boron carbide, Mater. Sci. Eng. A. 509 (2009) 89–93.
[16] H.-W. Kim, Y.-H. Koh, H.-E. Kim, Densification and mechanical properties of B_4C with Al_2O_3 as a sintering aid, J. Am. Ceram. Soc. 83 (11) (2000) 2863–2865.
[17] K.R. Gopi, R. Nagarajan, S.S. Rao, S. Mandal, Erosion model on alumina ceramics: a retrospection validation and refinement, Wear 264 (2008) 211–218.
[18] P.H. Shipway, I.M. Hutchings, The role of particle properties in the erosion of brittle materials, Wear 193 (1996) 105–113.
[19] C.M. Preece, N.H. Macmillan, Eros. Ann. Rev. Mater. Sci 7 (1977) 95–121.